Characteristics and evolution of heavy components in bio-oil from the pyrolysis of cellulose, hemicellulose and lignin

Dian Zhong, Kuo Zeng, Jun Li, Yi Qiu, Gilles Flamant, Ange Nzihou, Vasilevich Sergey Vladimirovich, Haiping Yang, Hanping Chen

Characteristics and evolution of heavy components in bio-oil from the pyrolysis of cellulose, hemicellulose and lignin

Dian Zhong [a], Kuo Zeng [a,b,*], Jun Li [a], Yi Qiu [a], Gilles Flamant [c], Ange Nzihou [d], Vasilevich Sergey Vladimirovich [e], Haiping Yang [a], Hanping Chen [a]

[a] State Key Laboratory of Coal Combustion, Huazhong University of Science and Technology, 1037 Luoyu Road, Wuhan, Hubei, 430074, PR China
[b] Shenzhen Huazhong University of Science and Technology Research Institute, Shenzhen, 523000, China
[c] Processes, Materials and Solar Energy Laboratory, PROMES-CNRS, 7 Rue du Four Solaire, 66120, Odeillo Font Romeu, France
[d] Université de Toulouse, Mines Albi, UMR CNRS 5302, Centre RAPSODEE, Campus Jarlard, F-81013, Albi, Cedex 09, France
[e] Institute of Energy, National Academy of Sciences of Belarus,·Akademicheskaya Str., 220072, Minsk, Belarus

Keywords:
Pyrolysis
Bio-oil
Heavy compound composition
FT-ICR-MS
KMD

A B S T R A C T

Three main components of biomass were pyrolyzed individually in a closed reaction system at 500–700 °C for 60s and 90s. Then bio-oil heavy compounds were further analyzed with Fourier transform-ion cyclotron resonance-mass spectrometry (FT-ICR-MS) and Kendrick mass defect (KMD) analysis. The evolution paths of heavy compounds for the different pyrolysis stages were proposed. It was found that the sugars and phenolic-like species in heavy compounds were the most active substances during secondary reactions. Moreover, the rising temperature promoted this secondary reaction of phenolic-like species as the decrease in their abundances growing from 13% to 54%, while contrarily inhibited it for hemicellulose as the decrease in their abundances changing from 44% to − 2%. The lignin-derived lipids and unsaturated hydrocarbons that generated in the secondary reactions increased with rising temperature. KMD analysis showed that the heavy compounds of cellulose and hemicellulose prefer homologous evolution during pyrolysis, while those of lignin had more complex evolution paths like cracking and recombination.

1. Introduction

Pyrolysis technique has been widely applied for bio-oil production from biomass like microalgae, wood, crop residues and other carbonaceous materials, which can be used as biofuel and as high value-added chemical products [1–3]. However, it has been reported that the composition of liquid products of biomass pyrolysis is very complex and chemically unstable due to the large number of heavy compounds [4]. Generally, the heavy compounds results in bio-oil condensation in the downstream pipeline during the production and utilization, which seriously deteriorates the working condition of the equipment, and causes additional production costs. In addition, the formation of heavy compounds is harmful to both the quantity and the quality of pyrolysis oil. Consequently, for a better utilization of bio-oil, it is important to clarify the composition and formation mechanism of the heavy compounds.

Pyrolysis of biomass is a complex physical and chemical process, which characteristics are closely related to the feedstock composition [5]. Biomass can be regarded as organic matter formed by cross-linking of three main components (cellulose, hemicellulose and lignin), therefore the pyrolysis process of biomass can be simplified as the superposition of the pyrolysis behavior of its three main components [6], which are different from each other [7]. Hence, the formation mechanism of bio oil and the heavy compounds can be derived from the evolution of the three main components of biomass during the pyrolysis process.

Cellulose has a relatively more regular structure among the three components. Therefore, the formation mechanism of cellulose bio-oil is now well developed, among which the model proposed by Bradbury and Shafizadeh (B-S model) is widely accepted [8]. According to this model, cellulose undergoes depolymerization and dehydration at a pyrolysis temperature below 300 °C, and is transformed into an intermediate called “active cellulose”. Most of the light compounds in cellulose pyrolysis are generated by the active cellulose, and several possible

* Corresponding author. State Key Laboratory of Coal Combustion, Huazhong University of Science and Technology, 1037 Luoyu Road, Wuhan, Hubei 430074, PR China.
E-mail address: zengkuo666@hust.edu.cn (K. Zeng).

Table 1
The proximate and ultimate analysis (dry basis, wt.%).

	Proximate analysis			Ultimate analysis					LHV (MJ/kg)
	V	FC	A	C	H	N	S	O[a]	
Cellulose	95.5	4.5	0.0	42.7	6.2	0.03	0.05	51.0	15.47
Xylan	76.8	21.4	1.8	41.6	5.7	0.02	0.03	52.6	15.31
Lignin	58.9	36.9	4.2	48.3	4.9	0.1	3.1	43.6	19.31

V represents volatile, FC represents fixed carbon, A represents ash.
[a] Calculated by difference. And V.

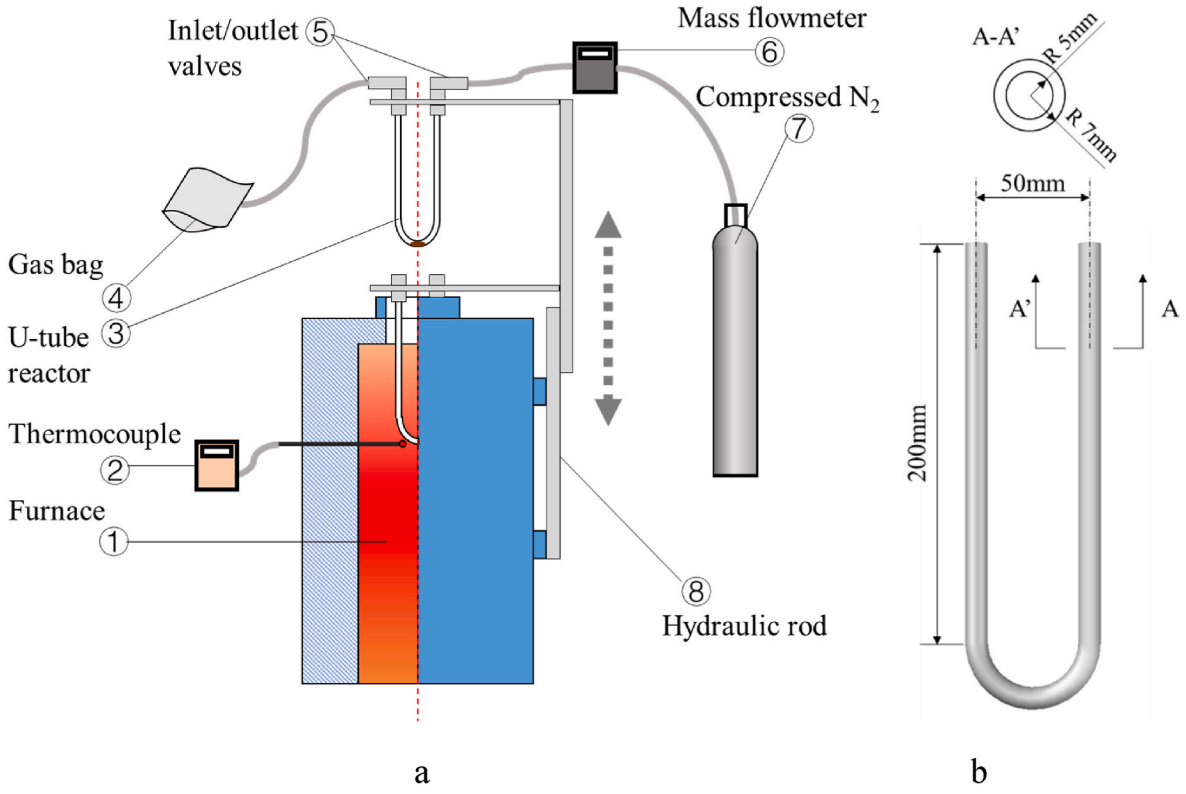

Fig. 1. The closed pyrolysis system (a) and the U-tube reactor (b).

pathways has been proposed 9. Mettler et al. [10] showed that oligosaccharides are more likely to produce furans, and under certain conditions the furan compounds are easily condensed to coke, which indicates a possible pathway of formation of heavy compounds. Lu [11] and Hosoya [12] found that levoglucan is thermally stable in the gas phase, while undergoes secondary reactions to generate coke and other heavy components in the liquid phase. Impressively, the pyrolysis experiments in Hosoya's works [12–14] were conducted with a closed ampoule reactor, which allows an easy control of the reaction process and reaction time.

The separation of hemicellulose from biomass is difficult to perform and this compound is unstable during pyrolysis due to its complex structure. Therefore, the pyrolysis mechanism of hemicellulose was less studied, and to overcome this problem xylan is commonly used as a model compound. Chen et, al [15]. found that the thermogravimetric behavior of xylan could be divided into the primary volatilization stage (210–340 °C) and the secondary stage (340–500 °C) corresponding to the intensive secondary reaction. Fisher et al. [16] compared the thermogravimetric behavior of cellulose and xylan, and found that xylan has a lower thermal stability but higher coke yield than cellulose, resulting an earlier peak of oil yield at 480 °C. Ponder et al. [17] explained that xylose molecules cannot exist stably through intramolecular dehydration to form glycosides due to the lack of one hydroxyl group. Further study showed that hemicellulose plays an important role in the formation of solid products and can be regarded as a potential precursor for the coke formation [18]. It also has a certain influence on the formation of heavy components during pyrolysis.

The pyrolysis of lignin starts at about 200 °C, and the decomposition continues as the temperature rises [19]. Kawamoto et al. compared the thermolysis behavior of 8 different lignin dimers, and found that the types of substituents on the aromatic ring and the connection ways between monomers affect the pyrolysis products [20]. Other studies found that monophenols and their derivations are easy to polymerize into products with larger molecular weight [21,22]. It has been proved that there are a lot of molecule with molecular weight in the range 200–1300 Da existing in the pyrolysis products of lignin, which cannot be analyzed by GC-MS [22,23]. All these data indicate that lignin is likely to generate heavy components.

Most of previous studies on bio-oil formation mechanism only focus on substances with small molecular weight using GC-MS, UV-F and FT-IR, which can not give the detail information of heavy compounds previously mentioned. Thus, the heavy compounds in bio-oil are less discussed so far because of the lack of appropriate analysis methods before Fourier transform-ion cyclotron resonance-mass spectrometry (FT-ICR-MS) has been introduced. The unique element composition of each substance can be given for further characterization thanks to its

Table 2
The rules applied in calculation.

Items	Rules	Reference
C number	$^{12}C \leq 50; ^{13}C \leq 2$	[44]
H number	$^{1}H \leq 100$; H/C ≤ 2.35	
O number	$^{16}O \leq 30$; O/C ≤ 2	
N number	$^{14}N \leq 5$;	
S number	$^{32}S \leq 2; ^{35}S \leq 1$	
Relative error (ppm)	≤3 ppm	[27]
Absolute error	$\leq 10^{-3}$	[39]
DBE (Double Bond Equivalent)	Positive integer	[45]
Others	N-rules	[46]

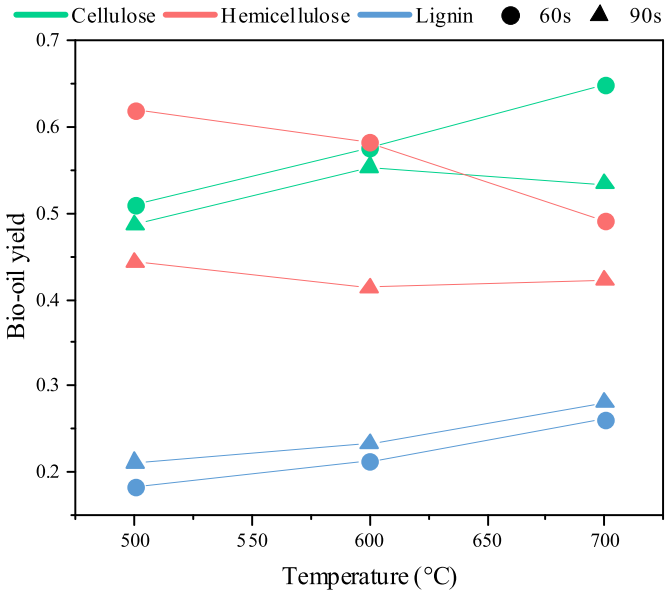

Fig. 2. The oil yields of three samples.

ultrahigh resolving power (>200,000) and wide detectable range of molecular weight (200–1000 Da). Consequently, the global composition of bio-oil has been studied with the help of FT-ICR-MS [24–26]. Xiong et al. [27,28] showed the pyrolysis behavior of bio-oil, and then assessed the chemical composition of heavy components derived from three main components of biomass (400–650 °C). They found that the oxygen-containing functional groups play an important role during the formation of heavy compounds. Xiao et al. [29] explored the formation mechanism of the oxygenated polycyclic aromatic hydrocarbons during cellulose pyrolysis. The formation of phenolic oligomers in the lignin-derived heavy compounds has also been studied [30]. Their works suggested that the formation processes of these heavy compounds differ from the three components of biomass, and is influenced by the temperature and heating rate.

In order to gain insights into the formation mechanism of these components, the Kendrick mass defect (KMD) method was applied to mass spectrometry analysis [31]. Qi et al. used FT-ICR-MS combined with 2D KMD plots to characterize lignin depolymerization products and showed the activities of different side-chains [32]. Dhungana et al. introduced KMD methods to compare the bio-oil from corn stover and pine shavings pyrolysis, and their differences on aliphatic chains can be visually observed from KMD plots [33]. Nevertheless, the composition as well as the evolution of heavy compounds from the three components of biomass pyrolysis remained unclear, and it is helpful to understand the formation mechanism of heavy oil and guide the upgrading process of bio-oil.

In this paper, the fast pyrolysis of cellulose, hemicellulose and lignin with 500,600 and 700 °C for 60s and 90s were conducted in a closed reaction system. FT-ICR-MS and KMD analysis was used to study the chemical composition and evolution of their heavy compounds.

2. Material and methods

2.1. Raw material

The cellulose sample (CAS 9004-34-6), xylan (CAS 9014-63-5) and alkali lignin (CAS 8068-05-1) were dried at 105 °C for 4 h before used. Xylan was used as the alternative of the hemicellulose in this paper. The proximate and elemental analysis of the three components is shown in Table 1. N and S contents in lignin are significantly higher than in the other two components, while the oxygen content is relatively lower. This difference has a great impact not only on the subsequent data processing but also on its pyrolysis behavior.

2.2. Pyrolysis experiment

The experiment was conducted in a closed reaction system shown in Fig. 1a. The system includes a vertical tube furnace (OTF-1200X-4-VTQ) and a quartz U-tube reactor. The specific size of the reactor is shown in Fig. 1b.

Before pyrolysis, 100 mg sample was loaded in the U-tube reactor, and then the system was flushed by N_2 (99.999%, 300 ml/min) for 3 min. The thermocouple was placed at a depth of 250 mm from the entrance of the furnace to measure the temperature of reaction zone. Once the target temperature is reached (500 °C, 600 °C, 700 °C), the gas inlet and outlet valves were closed, and the reactor was quickly lowered down for pyrolysis during 60s/90s. Hosoya and Jiang [14,34] proved that the secondary reactions mainly take place after 60s for pyrolysis of a small amount (100 mg) of cellulose and lignin, and that the pyrolysis is nearly completed after heating for 90s or longer. Thus, the reaction time were set as 60s and 90s, representing the primary pyrolysis and secondary pyrolysis respectively.

After pyrolysis, the reactor was taken out immediately and cooled with compressed air for 2 min and subsequently immersed in ice-water mixture for 1 min. Then the valves were open again and uncondensed gas was wiped out by N_2 (99.999%, 300 ml/min) for 3 min and gathered by gas bag. The liquid products condensed in the reactor was extracted with CH_3OH to give a 10 ml solution. The dark-colored residue that can not be dissolved and the solid product were defined as char fraction in this paper.

2.3. Analysis and characterization of bio-oil

2.3.1. GC-MS setting

The bio-oil were analyzed using gas chromatography-mass spectrometry system (GC/MS, Agilent 7890B/5977A, America). Capillary column model is DB-5MS (30 m × 0.32 mm × 0.25 μm), The oven temperature program was as follows: initial temperature of 50 °C, increase to 100 °C at 10 °C/min, increase to 200 °C at 5 °C/min, increase to 300 °C at 10 °C/min, and hold for 3 min. The inlet temperature was 280 °C, the split flow rate was 40 ml/min, the split ratio was 40:1, the mass spectrometry ionization mode was EI (70 V). The results were compared with the NIST 14 database, and the m/z scanning range was 35–550.

2.3.2. FT-ICR-MS analysis

FT-ICR-MS (Bruker, Solarix 7.0 T) was used to analyze the heavy compounds in oil in negative mode using electrospray ionization (ESI) source. The ionization method of FT-ICR-MS has a preference for different target components based on their characteristics like different functional groups, aromatic content, and polarity. Among these soft ionization methods, ESI (electrospray ionization) and APPI (atmospheric pressure photoionization ionization) are mostly used in analyzing biomass pyrolysis oil for their wide range of application [22,

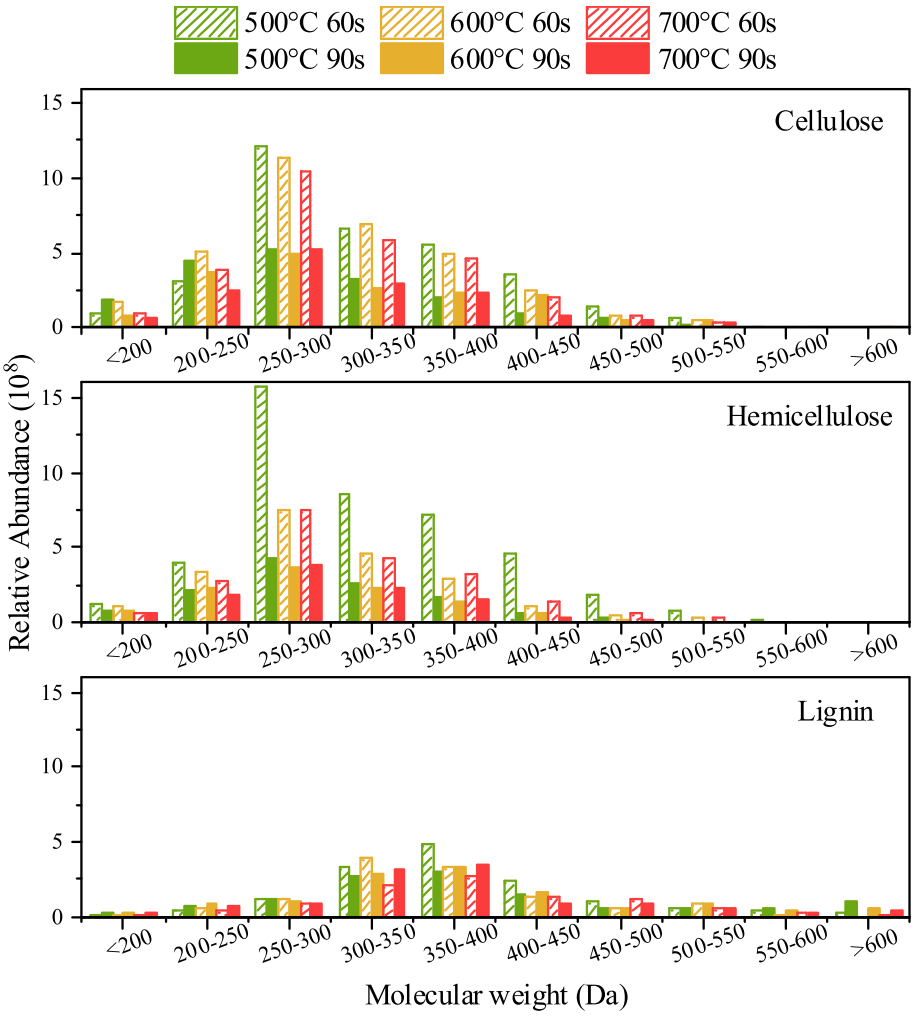

Fig. 3. The distributions of the heavy components of three samples produced at 500, 600 and 700 °C under 60s and 90s pyrolysis time.

Table 3
The percentages of different O-containing species in heavy compounds in cellulose-oil (C), hemicellulose-oil (H) and lignin-oil (L) produced at 500, 600 and 700 °C for 60s and 90s.

Sample	Content (%)				
	ON = 0	1 < ON < 3	4 < ON < 6	7 < ON < 9	ON > 9
C-500-60	5.7	10.0	35.2	34.1	15.0
C-500-90	1.6	9.1	49.3	31.8	10.2
C-600-60	2.2	9.7	33.1	39.1	14.9
C-600-90	3.1	14.5	42.1	30.2	10.1
C-700-60	4.3	12.3	33.2	37.2	13.0
C-700-90	4.6	14.7	37.1	32.1	11.5
H-500-60	2.2	4.6	33.8	42.7	16.7
H-500-90	2.9	6.2	40.1	38.5	12.3
H-600-60	0.2	6.9	43.5	39.3	10.1
H-600-90	2.7	11.3	42.9	33.3	10.8
H-700-60	1.4	16.2	36.2	29.2	17.0
H-700-90	4.1	13.7	39.6	30.5	12.1
L-500-60	18.5	39.2	29.6	12.0	1.1
L-500-90	17.1	38.5	34.3	9.1	1.0
L-600-60	17.6	34.7	31.8	13	1.9
L-600-90	15.4	40.0	33.7	9.7	1.2
L700-60	17.1	40.2	31.0	9.8	1.9
L-700-90	13.3	45.5	33.2	5.3	2.7

27,28,35–39]. Considering that the bio-oil is generally acidic and oxygen-contained, the ESI ionization source which is more sensitive to polar substances was chosen [40]. Furthermore, the negative ion mode ($ESI^{(-)}$) was chosen instead of the positive one ($ESI^{(+)}$) because the bio-oil obtained from model compounds has little nitrogen and sulfur, which are preferred by $ESI^{(+)}$ [39]. The details of basic instrument setting have been mentioned in our previous study [39]. Before analysis, the bio-oil was diluted with CH_3OH (LC/MS grade) to 0.4 mg/ml for a better ionization and separation in the FT-ICR-MS [39,41,42], and the instrument was calibrated by NaCOOH solution [43]. Then the sample was infused into the MS at a rate of 120 μml/h. Each spectrum was gained after co-adding 128 scans to enhance the signal-to-noise ratio (S/N).

After testing, those signal with a S/N ≥ 3 were selected [28] for further calculation using MATLAB script [39] and their chemical formulas were determined by several rules listed in Table 2. Besides, the solvent used to dilute the oil sample was also analyzed, and the prominent signals in solvent mass spectrum were abandoned in the experiment results.

2.3.3. KMD analysis

FTMS gives the relative molecular mass (RM) of each molecule, which takes the 12C (12.000000 Da) as the mass reference. Replace the 12C with a certain group F, then the relative molecular Mass RM of a molecule will be transformed into Kendrick Mass (F) (Kendrick Mass taking F group as the mass reference, KM(F)) shown as Eq (1) [47]:

$$KM(F) = RM \times \frac{NM_F}{RM_F} \quad (1)$$

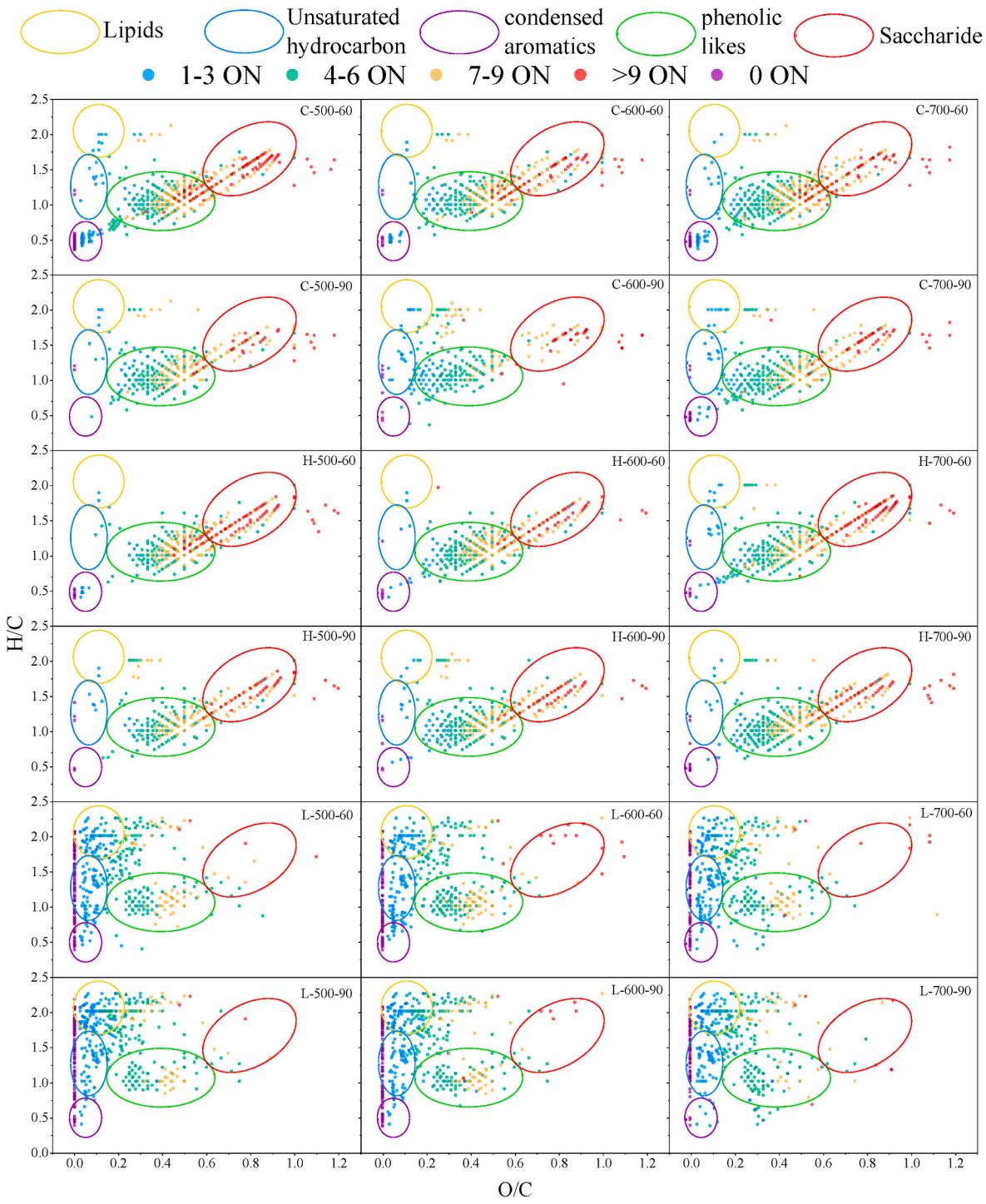

Fig. 4. The van Krevelen plots of heavy components in cellulose-oil (C), hemicellulose-oil (H) and lignin-oil (L) where first letter represents feedstock, first number represents temperature (°C) and second number represents reaction time (s).

where, RM_F is the relative molecular weight of the F group, and NM_F is the relative molecular weight of the F group after rounding. For example, $RM_{CH2} \approx 14.01565$, $NM_{CH2} = 14$.

It follows that a series of homologues with the same characteristic structure will have identical Kendrick mass defects [47]:

$$KMD(F) = KM(F) - NM \tag{2}$$

where the KMD(F) represents the Kendrick mass defect on the basis of F group, and NM represents the rounded relative molecular weight.

The existence of molecules with the same KMD in the pyrolysis products indicates that such substances have undergone the removal or addition of F group during the pyrolysis process [47–50]. Therefore, the evolution of heavy components can be explored by analyzing the KMD of different groups [51].

3. Results and discussion

3.1. Bio-oil yield and macroscopic characteristics of heavy compounds

The trend of bio-oil yield under different reaction time is basically

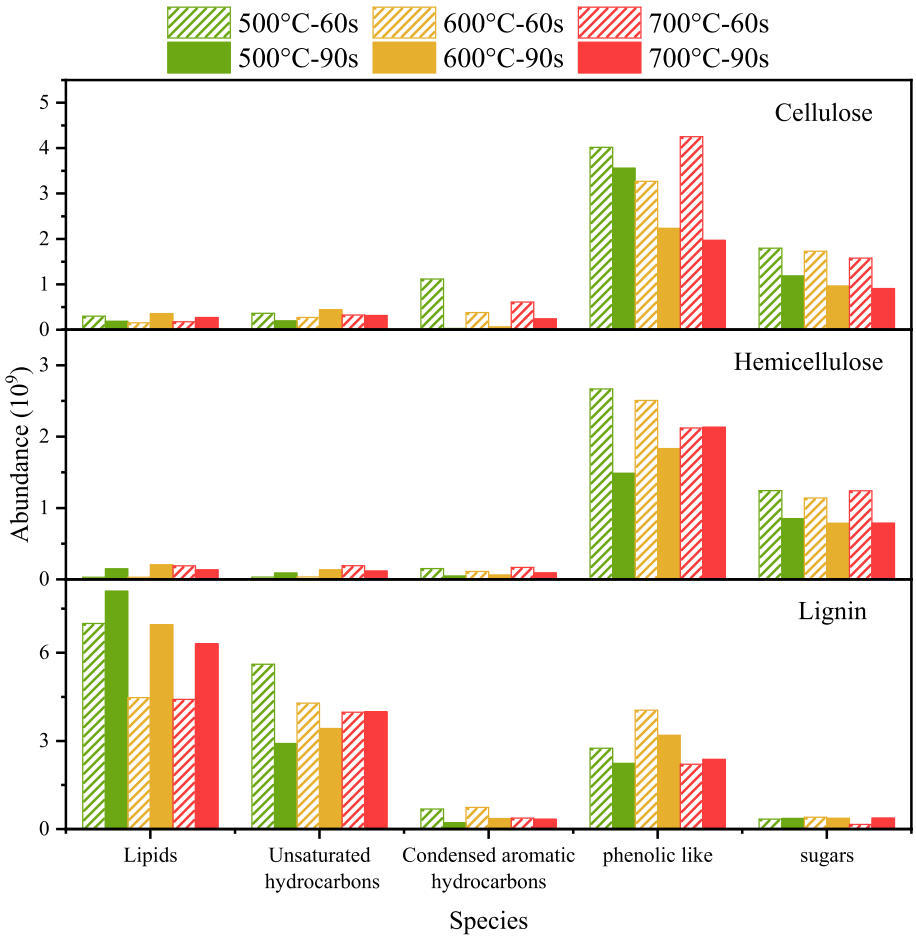

Fig. 5. The abundances of different species in the heavy compounds derived from three components.

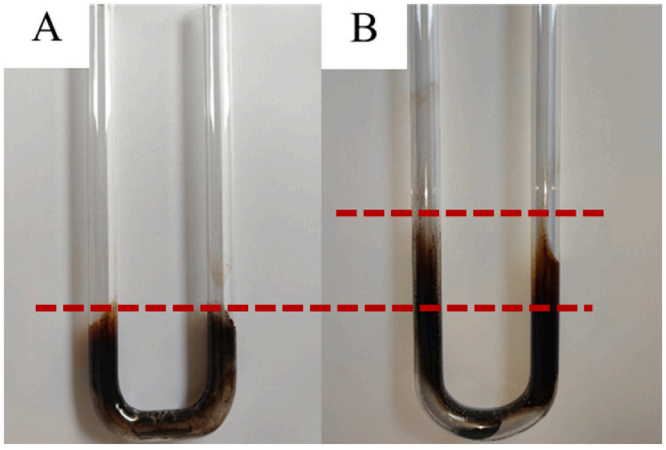

Fig. 6. The coke formation of cellulose pyrolysis if different reaction stages: A is 600 °C, 60s pyrolysis; B is 600 °C, 90s pyrolysis.

the same as temperature rises as shown in Fig. 1. The oil yield of cellulose was generally the highest, followed by those of hemicellulose and lignin. The oil yields of cellulose and hemicellulose decreased with the increase of reaction time, indicating that the secondary reaction would reduce the yield of bio-oil [52,53]. The oil yield of lignin increased with the increase of reaction time, possibly because the secondary stage of lignin pyrolysis tends to promote the formation of liquid products [14]. The oil yield of cellulose pyrolyzed for 60s continually increased as temperature rose from 500 °C to 700 °C, While it slightly decreased at 700 °C for longer pyrolysis time, which is consistent with the results of Shen et al. [53]. With the increase in temperature, the content of levoglucan in bio-oil gradually decreased due to the secondary reactions. The lignin-derived oil yield steadily increased at higher temperature, while the hemicellulose-derived oil yield tended to decrease. Same results can also be observed in other works [54].

The distributions of molecular weight of heavy compounds in cellulose and hemicellulose have the highest abundance in a range of 250Da–300Da (Fig. 3). The molecular weight of heavy compounds in lignin concentrated on the range of 300Da–400Da, and its total abundance of heavy compounds was less than in others. Fig. 3 also shows that the temperature and reaction time affect the molecular weight distribution of the heavy components. The abundance of heavy oil produced from cellulose and hemicellulose in the primary pyrolysis stage was significantly greater than that in the secondary pyrolysis stage particularly in a range of 250Da–450Da. These differences between the two stages shrunk with the increase in temperature. These could be mainly caused by the differences of the total oil yield (Fig. 2). However, the abundance of lignin-derived heavy compounds changed more slightly with the increase of pyrolysis time compared with the others. The abundance of compounds with a higher molecular weight (>600Da) increased significantly with temperature rising from 500 to 700 °C, which indicated that these larger compounds of lignin was more likely produced in the secondary reaction stage.

Xiong et al. found the oxygen-containing species participated in the formation of most heavy compounds. The changes of oxygen content in heavy oil at different reaction stages is shown in Table 3 according to Eq. (3).

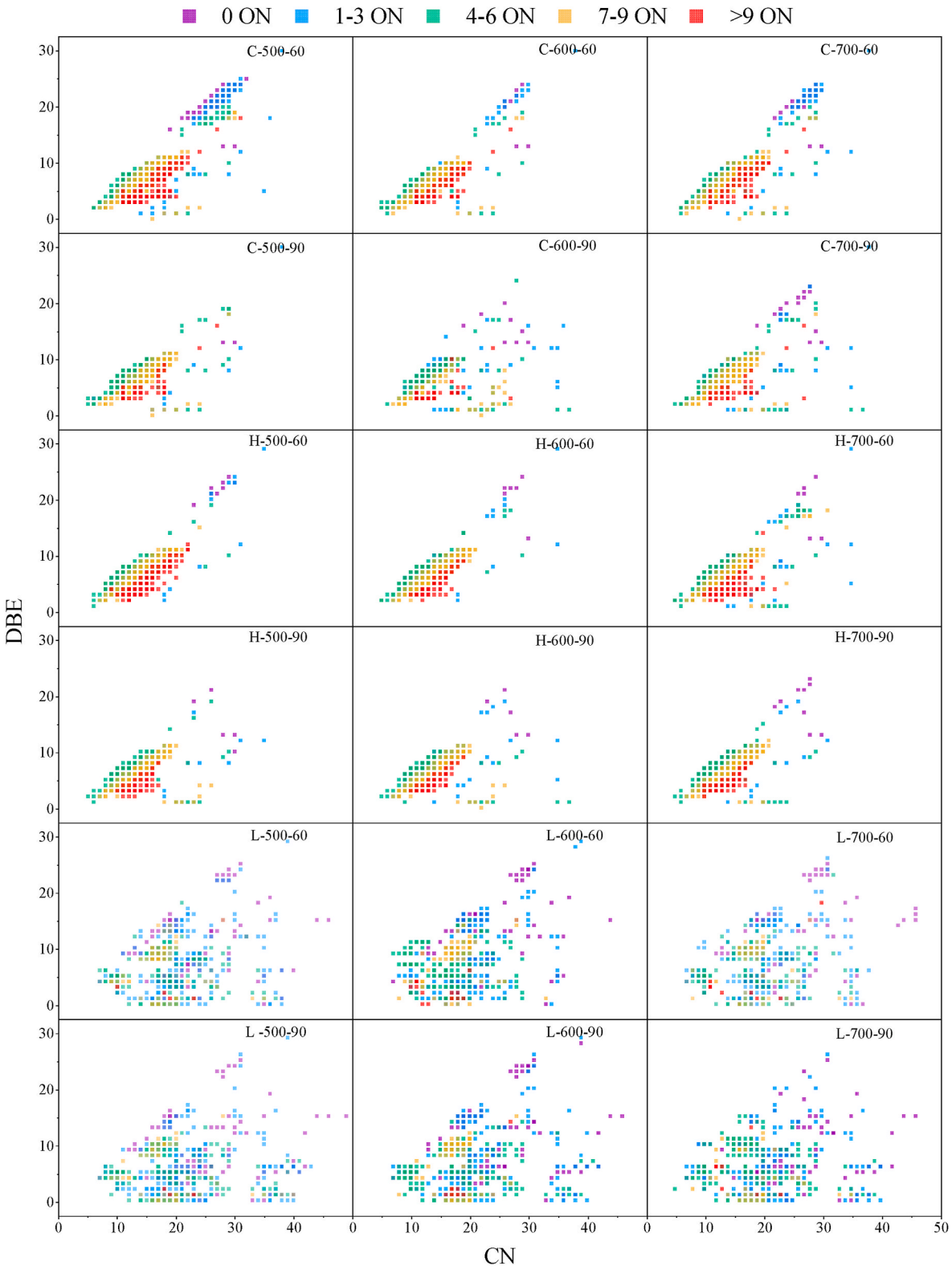

Fig. 7. The DBE distribution with CN of cellulose-oil (C), hemicellulose-oil (H) and lignin-oil (L) pyrolyzed at 500, 600 and 700 °C for 60s and 90s.

$$C_{ON=x} = \frac{\sum I(O_x)}{\sum I} \tag{3}$$

where the $C_{ON=x}$ represents the relative content of the compounds with x oxygen atoms, I is the peak abundance of each molecular, and $I(O_x)$ is the peak abundance of molecular with x oxygen atoms.

The increase of reaction time results in the decrease of the content of almost all substances with oxygen number (ON) greater than seven. More substances with lower oxygen content was generated. However, the substances without oxygen atoms in lignin showed a slight decrease in the second reaction stage. According to the classification based on H/C and O/C, the substances that do not contain oxygen are mainly lipids,

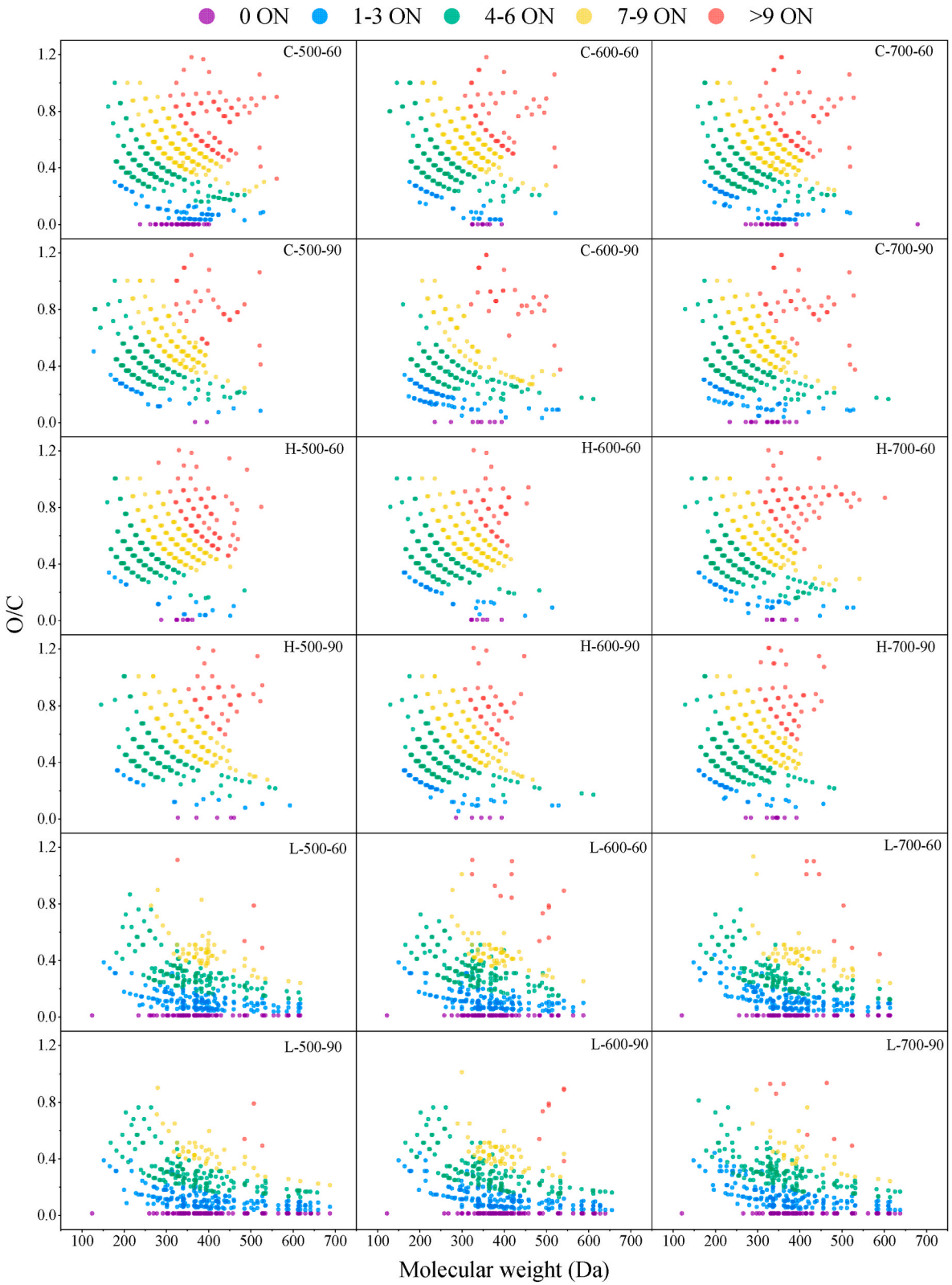

Fig. 8. The O/C distribution with molecular weight of cellulose-oil (C), hemicellulose-oil (H) and lignin-oil (L) produced at 500, 600 and 700 °C for 60s and 90s.

unsaturated hydrocarbons and condensed aromatic hydrocarbons. This indicates that the secondary reaction has an inhibitory effect on the generation of these substances, but the details still needed further studies.

3.2. Characteristics of heavy compounds

3.2.1. Distribution of species in heavy compounds

The van Krevelen plot shows the H/C ratio versus O/C ratio of each compound. Previous studies concluded that the distributions of species in bio-oil correspond to unique constant regions on the van Krevelen

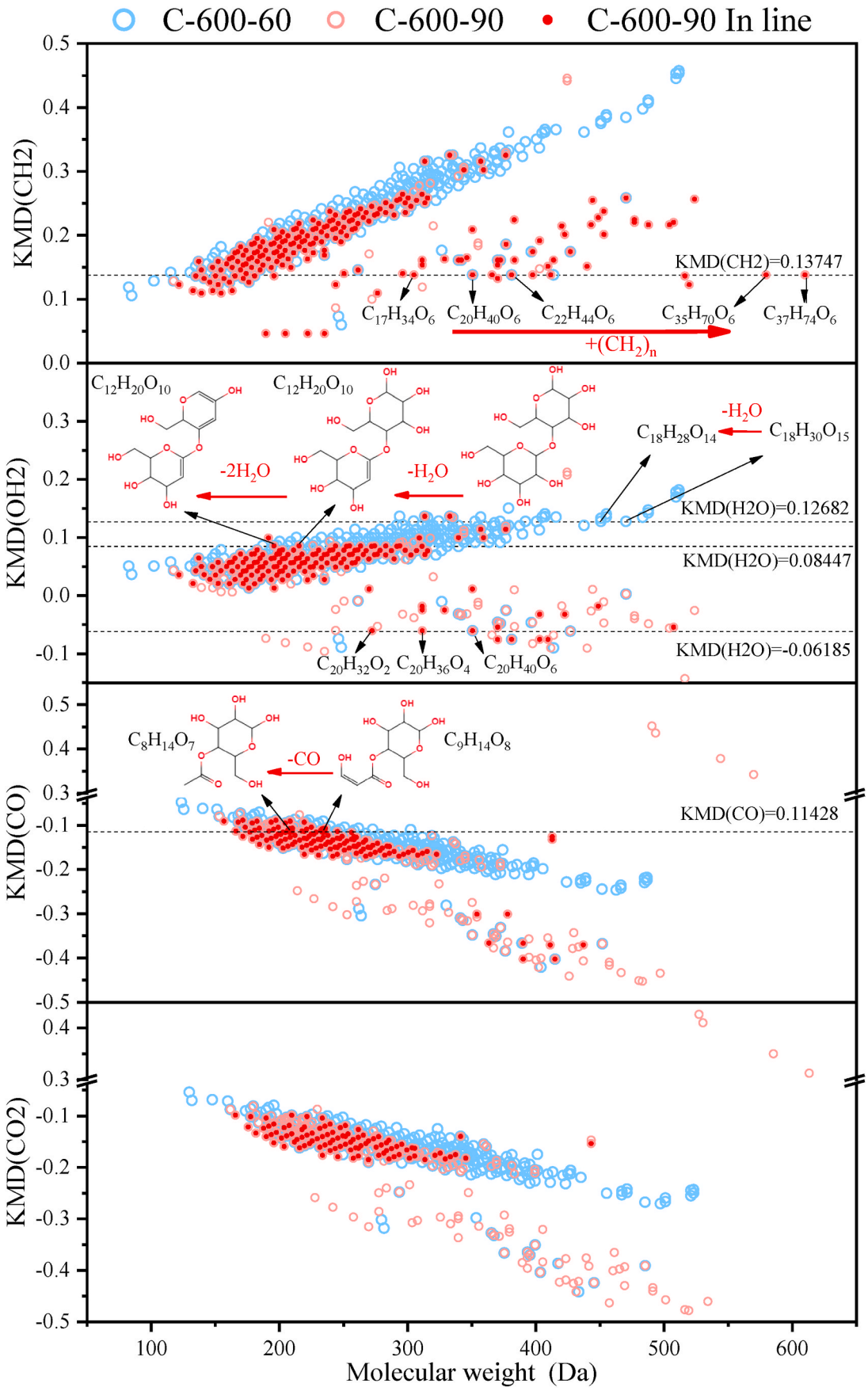

Fig. 9. KMD based on different groups of heavy compounds in cellulose pyrolysis oil.

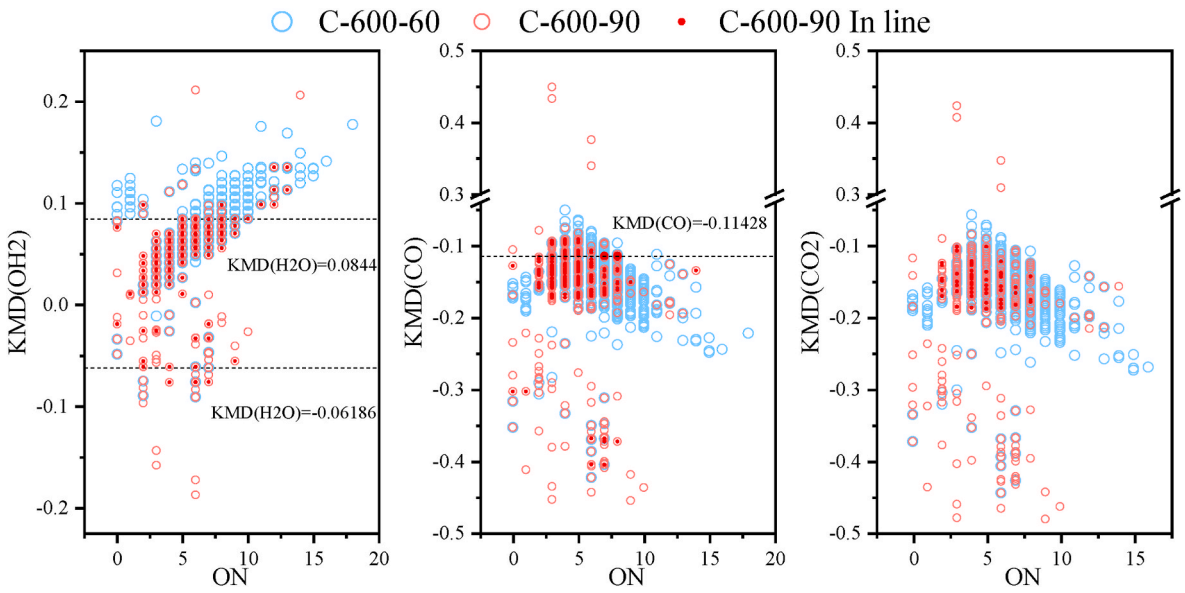

Fig. 10. KMD of oxygen-containing compounds in cellulose pyrolysis oil.

plot. They are generally classified as lipids ($0 \leq O/C \leq 0.2$, $1.7 \leq H/C \leq 2.25$), unsaturated hydrocarbons (UHs, $0 \leq O/C \leq 0.1$, $0.7 \leq H/C < 1.7$), condensed aromatic hydrocarbons (CAHs, $0 \leq O/C \leq 1.0$, $0.3 \leq H/C \leq 0.7$), phenolic-like species ($0 \leq O/C \leq 0.6$, $0.6 \leq H/C \leq 1.3$) and saccharides (sugars, $0.5 \leq O/C \leq 0.9$, $1.2 \leq H/C \leq 2.25$) [24,36,42,55,56].

The heavy compounds were classified according to the number of oxygen atoms and presented on van Krevelen diagram, as shown in Fig. 4. The heavy compounds of cellulose and hemicellulose were mainly distributed in the regions of sugars and phenolic-like species, but less in the lipids, unsaturated hydrocarbons and condensed aromatic hydrocarbons regions. All kinds of Oxygen-containing species, especially those with 4–9 ON are found in phenolic-like region, while the sugars are mainly substances with ON greater than 7. It meant that these components were produced by the depolymerization of various polysaccharide precursors [57]. The distributions of lignin heavy compounds were different from those of another two samples in both elemental composition and compounds distribution. The heavy compounds of lignin were more abundant than those of cellulose and hemicellulose, and mainly distributed in the regions of lipids, unsaturated hydrocarbons, condensed aromatic hydrocarbons and phenolic-like species in Fig. 4. Almost no saccharides are generated. Although lignin is composed of various methoxy p-hydroxyphenyl propane, its main heavy components were lipids and unsaturated hydrocarbons whose maximum abundances account for 58.59% and 29.62%, rather than phenolic substances. On the contrary, a lot of "phenolic-like species" were generated in the heavy compounds of cellulose and hemicellulose whose origin structure does not contain any benzene ring. Lignin having more side chains, it generates more saturated/unsaturated free radicals during the pyrolysis process. These radicals can further recombine and form unsaturated hydrocarbons and lipid substances [28]. "Phenolic-like species" in the heavy compounds of cellulose and hemicellulose can only be derived from the recombination of small unsaturated radicals generated during pyrolysis or the derivatives of sugar units with large degree of unsaturation and ring structure formed through multi-stage dehydration, such as 1,4:3, 6-dihydro-α-d-glucopyranose ($C_6H_8O_4$) [58].

With the increasing of reaction time, the sugars and phenolic-like species in heavy compounds of cellulose reduced, and so did their abundances. The dehydration of sugars happened at a low temperature (550 °C), during which "phenolic-like species" were produced [59]. As the reaction time goes on, those species undergo secondary reaction like ring opening and cracking. It results in the formation of more kinds of derivatives and saturated/unsaturated hydrocarbons radicals with small molecular weight [28,59]. The abundance difference between two reaction times became larger with the increase in temperature (abundance reduced by 13% at 500 °C and by 54% at 700 °C). This trend suggests that the rising temperature promote the secondary reaction of sugars and phenolic-like species. This also explained the lower abundances of these two compounds at higher temperature for longer reaction time. The contents of lipids and unsaturated hydrocarbons for 60s pyrolysis were lower than for 90s at 600 and 700 °C. This finding suggests that higher temperature promotes the formation of lipids and unsaturated hydrocarbons in secondary reaction. Meanwhile, the content of condensed aromatic hydrocarbons decreased during secondary reactions, but the abundance of these compounds from 90s pyrolysis increased with temperature. This suggests that higher temperature inhibits the decrease of condensed aromatic hydrocarbons. Xiao et al. [29] proved that most of condensed aromatic hydrocarbons could be generated during secondary reaction of cellulose pyrolysis by Diels-Alder reaction, explaining the final increase of condensed aromatic species.

The heavy compounds of hemicellulose mainly distribute in the phenolic and saccharide regions that is similar to the results of cellulose. With the rise of temperature, both of them produce more phenolic-like species with $O/C < 0.3$, and show a trend of condensation. This suggests that the increase of temperature promotes the condensation by removing their oxygen-containing functional groups. However, hemicellulose generates more phenolic-like species and sugars in the primary stage, possibly because of its intensive depolymerization process [60]. With the increase of temperature, the phenolic-like species generated from the 60s pyrolysis decrease and the secondary decomposition process weakened, leading to the lower difference between the two stages (abundance reduced by 44% at 500 °C and by −2% at 700 °C). Meanwhile, the weakening decomposition also provides less pyrolytic radicals needed in the formations of lipids and unsaturated hydrocarbons. This trend explains their abnormally decrease at 700 °C in secondary pyrolysis. It can be speculated that lipids and unsaturated hydrocarbons can be formed by recombination of small radicals in both primary and secondary pyrolysis, while being further decomposed in secondary reaction. Temperature indirectly affects their formation by promoting or inhibiting the radicals generated from the secondary reaction of phenolic-like species and sugars.

Fig. 5 indicates that the increase of temperature inhibits the formations of lipids and unsaturated hydrocarbons in the lignin-derived heavy compounds in the initial pyrolysis. However, it promotes their formation

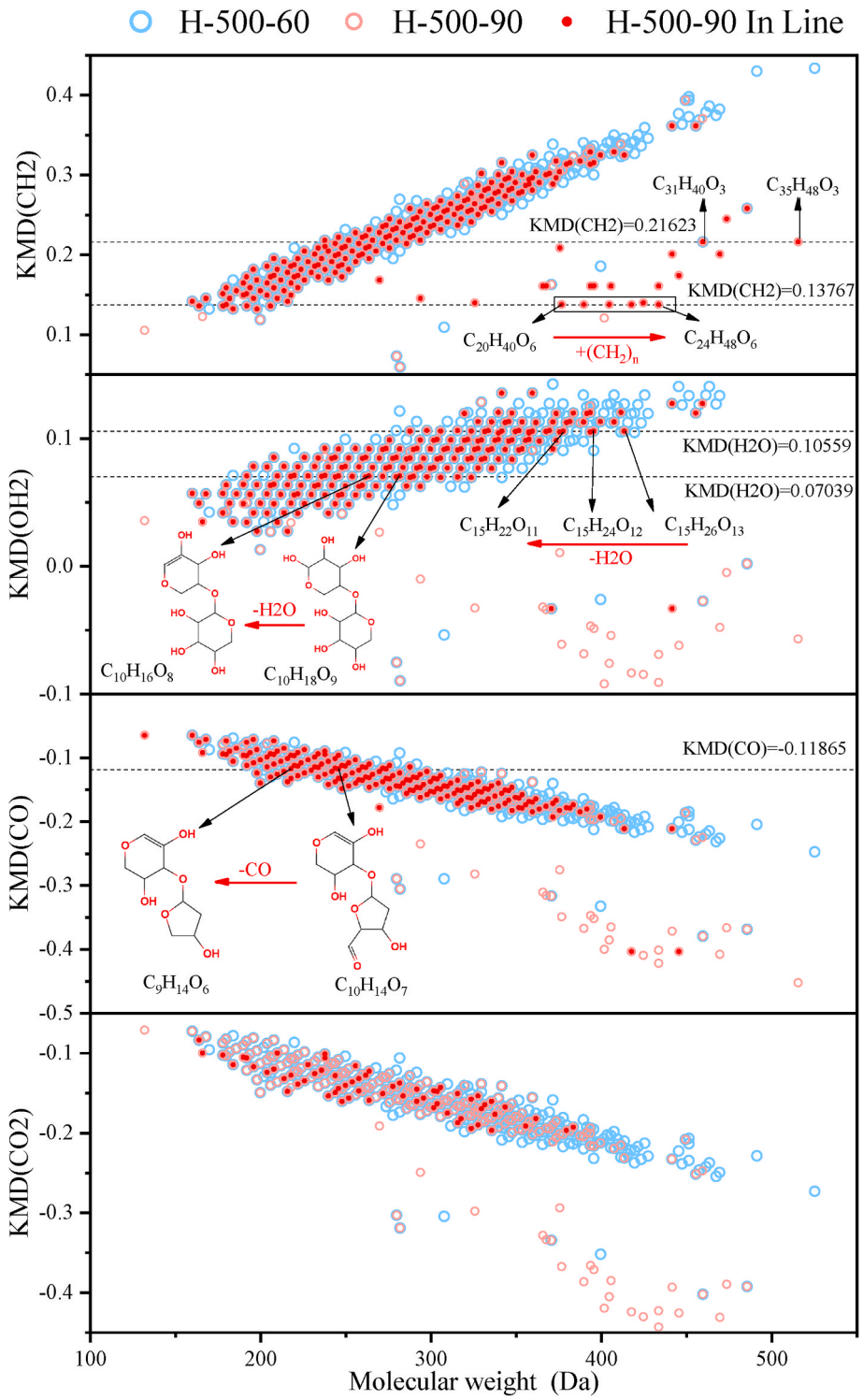

Fig. 11. KMD based on different groups of heavy compounds in hemicellulose pyrolysis oil.

during the secondary reactions and even overcame the secondary decomposition of unsaturated hydrocarbons leading to the increase of its abundance after 90s pyrolysis. The side chains on the lignin units begins to be remove at 400 °C [61], and the removal reaction tends to be completed with the increase of temperature. Therefore, it is speculated that the formation of lipids and unsaturated hydrocarbons are in competition at 700 °C leading to the weakening of the promoting effect of the secondary reaction of lipids. In the secondary reaction stage, phenolic substances will be further decomposed and transformed, making their content slightly lower. Meanwhile, those phenolic substances from lignin pyrolysis also acted as the precursors of the condensed aromatic hydrocarbons, which produced more condensed aromatic hydrocarbons compared to cellulose and hemicellulose.

3.2.2. *Characterization of DBE of heavy compounds*

In the DBE/CN diagram (Fig. 7) of cellulose and hemicellulose, the substances with different ON show obvious “layered” distribution, especially for the 60s pyrolysis. It shows that substances with high ON

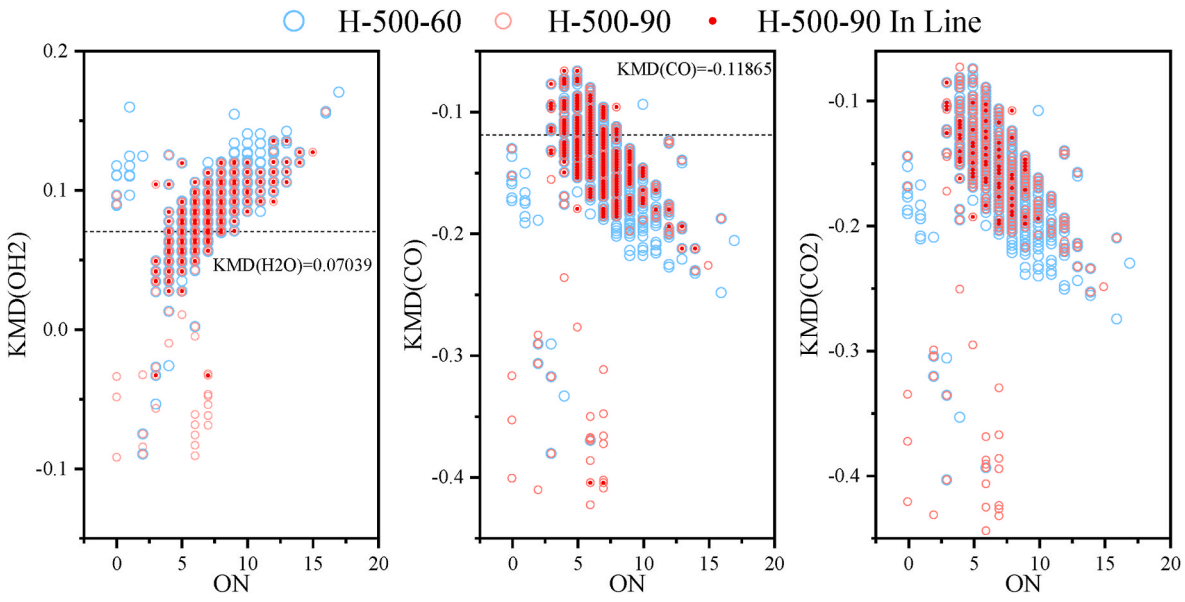

Fig. 12. KMD of oxygen-containing compounds in hemicellulose pyrolysis oil.

generally have low DBE/CN, indicating that oxygen-containing functional groups play an important role in the formation of heavy components [28]. Moreover, a "special island" can be observed in the 60s pyrolysis diagram, which is consisting of condensed aromatic hydrocarbons and unsaturated hydrocarbons with DBE >15, CN > 20 and ON<6. This clearly separated distribution indicates that two reaction path ways for the formation of heavy compounds in primary pyrolysis stage of cellulose are possible. One corresponds to the production of unsaturated macromolecules with low oxygen content such as condensed aromatic hydrocarbons, and the other one is related to the generation of pyrolytic derivatives of sugars and phenolic-like species with higher oxygen content.

With the increase of time, the DBE distribution tends to "collapse": many species in the "special island" (unsaturated hydrocarbon and condensed aromatic hydrocarbon) disappear, while some substances with DBE less than 15 and CN more than 20 are generated. It is worth noticing that less abundance and fewer species of condensed aromatic hydrocarbons (also shown in Figs. 4 and 5) may not be due to their decomposition in the second reaction. It could be the result of further polycondensation and transfer into secondary coke with longer pyrolysis time, which cannot be dissolved and detected. This can be supported by comparing the coke formed on the inner wall of the reactor after pyrolysis, as shown in Fig. 6. In addition, the substances with ON > 9 and DBE ≈5 gradually disappear with an increase of reaction time, which corresponds to the results shown in Fig. 4. Generally, the unsaturation of heavy components tends to reduce as the reaction proceeds. Considering the decrease of high ON species in longer reaction time, it is speculated that more decarbonylation reactions happen in the secondary reaction of cellulose-derived heavy compounds. Individually, hemicellulose produces less substances of the "island" in the primary stage than cellulose indicating that the condensation of hemicellulose is by far inferior to cellulose. With the rise of pyrolysis temperature, the change between the two stages gradually decreases, which indicates that the pyrolysis of hemicellulose is accelerated by temperature and the secondary reactions are promoted. As the reaction time goes on, more long-chain hydrocarbons with smaller DBE appear in the lignin pyrolysis heavy oil (Fig. 7) that are the corresponding lipids. For lignin-derived compounds, phenolic-like species with ON > 6 and CN of 15–20 in the primary stage are further replaced by the same species with lower ON accompanying with deoxidization in the secondary reaction.

3.2.3. Changes of O/C with molecular weight of the heavy components for different reaction times

As shown in Fig. 8, the compounds with O/C < 0.3 or >0.8 have the largest molecular weight for 60s pyrolysis of cellulose and hemicellulose. For 90s pyrolysis, the O/C ration of the compounds with large molecular weight are generally less than 0.2. It is more obvious in the lignin-derived heavy compounds that these large molecular are produced by the growth of lipids, unsaturated hydrocarbons and condensed aromatic hydrocarbons in the secondary reaction consistent with the distributions of DBE of the three samples. Supported by previous results, one can assume that the heavy components undergo deoxidation reactions such as decarboxyl, decarbonyl, dehydration and other reactions [27] during their formation.

3.3. KMD analysis of heavy compounds

3.3.1. Distributions of heavy compounds in KMD diagram

The formation and evolution of three kinds of heavy compounds were different because of their unique pyrolysis behavior, in which the oxygen-contained functional groups played an important role. The results of pyrolysis at characteristic temperature of each samples are selected for KMD analysis based on CH_2, H_2O, CO_2 and CO, etc, to reveal the evolution of heavy compounds. Considering the heavy oil yield and the intensity of secondary reaction, 500, 600 and 700 °C are chosen as the characteristic temperatures of hemicellulose, cellulose and lignin respectively.

Before discussing the evolution route based on the reaction time by KMD analysis, it is necessary to investigate the characteristic KMD distributions of the five kinds of species in three heavy oil samples based on CH_2 group (Fig. S1). It can be found that most of heavy components of both cellulose and hemicellulose are concentrated around a linear region ("main line" for short). This region contains saccharides, phenolic-like species, condensed aromatic hydrocarbons and parts of unsaturated hydrocarbons, while other parts of unsaturated hydrocarbons and lipids are found outside the region. Although the distribution of lignin-derived heavy compounds in the KMD diagram is quite different from that of cellulose and hemicellulose, the "main line" can still be distinguished.

3.3.2. Evolution of cellulose-derived heavy compounds

Fig. 9 shows the distribution of KMD with molecular weight based on CH_2, H_2O, CO and CO_2 groups. The two pyrolysis stages are distinguished by circles with different colors, and the homologues of the new

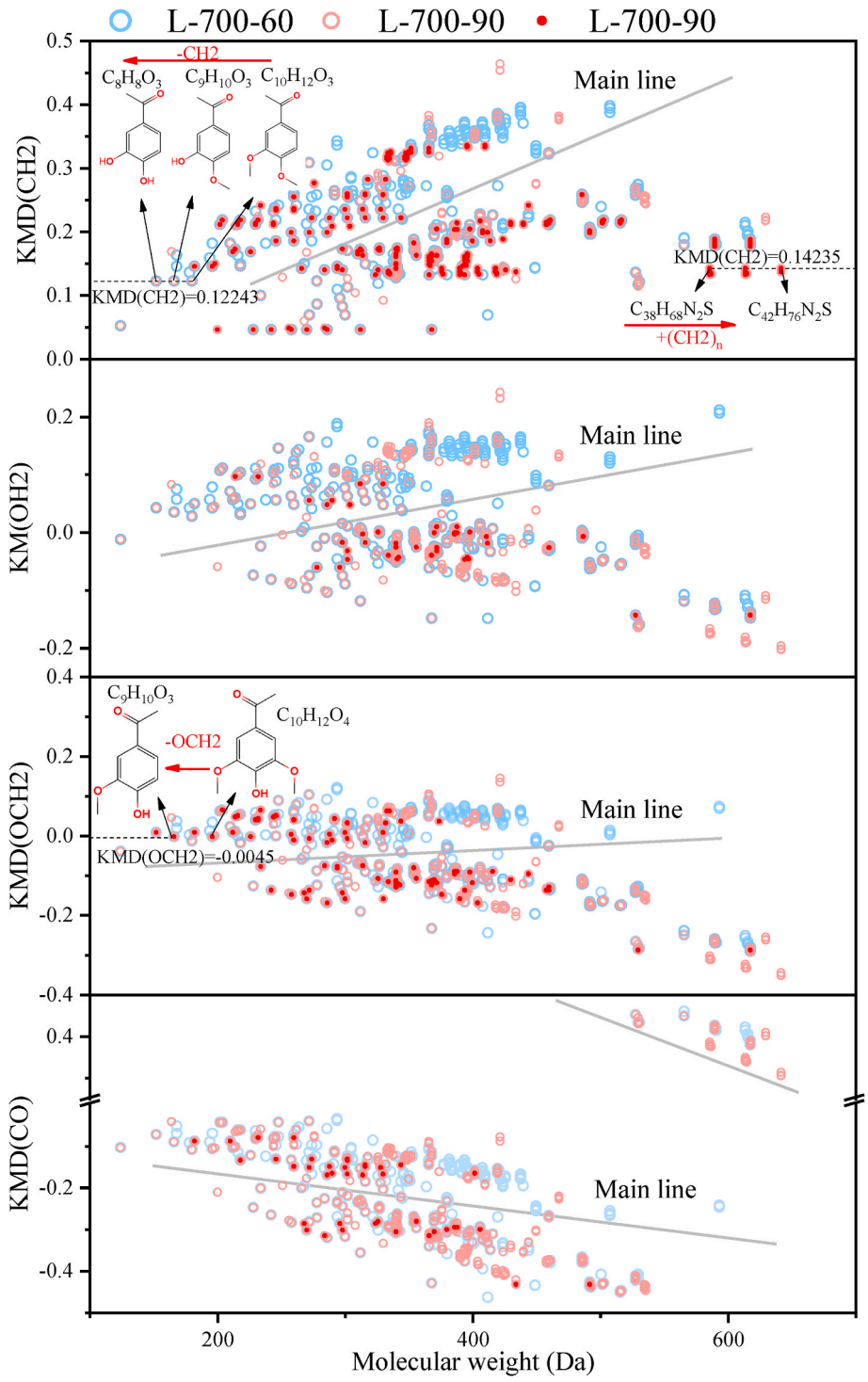

Fig. 13. KMD based on different groups of heavy compounds in lignin pyrolysis oil.

products generated in the second stage are represented by solid points. Combined with the species distribution in Fig. S1, it appears that the heavy components of cellulose mainly undergo the transformation between sugars, phenolic-like species and condensed aromatic hydrocarbons in the primary reaction stage. Some products in the primary reaction stage disappear with the increase of reaction time, while many new substances are produced in the secondary reaction stage.

The KMD(CH2) diagram indicates that most of the new substances (lipids and unsaturated hydrocarbons) outside the "main line" are generated in the secondary reaction stage. These substances are homologues of CH_2 group including some high molecular weight substances such as $C_{37}H_{74}O_6$. This indicates that in the secondary reaction stage, the newly generated lipids and unsaturated hydrocarbons are produced through the growth of alkane chains. The KMD(H2O) diagram reveals that the multi-stage dehydration reactions happen in some substances existing only in the primary stage which was also can be deduced from the van Krevelen diagram based on Stankovikj's work [62]. For example, the trisaccharide units $C_{18}H_{30}O_{15}$ dehydrated into $C_{18}H_{28}O_{14}$ detected by FTMS as shown in Fig. 9. More sugar units as well as some oxygen-containing lipids and unsaturated hydrocarbons

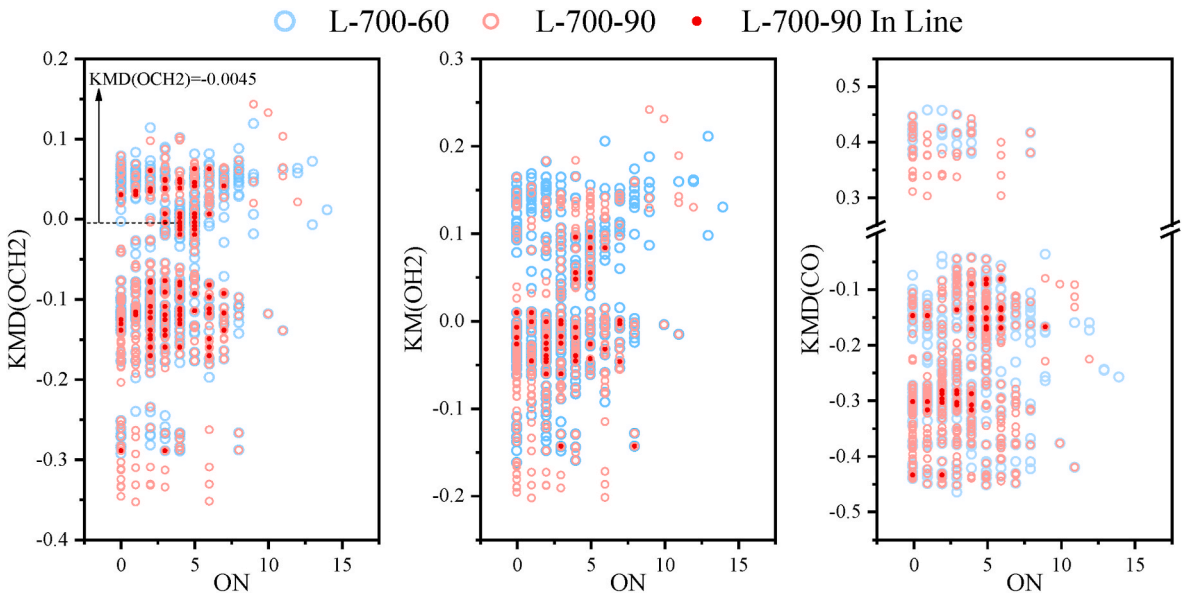

Fig. 14. KMD of oxygen-containing compounds in lignin-oil.

undergo deeper dehydration in the secondary reaction stage. The KMD (CO) diagram indicates a deep decarbonylation reaction in the secondary reaction stage for sugars. Taking the glucose dimer derivative ($C_9H_{14}O_8$) detected by GCMS and FTMS as an example, its carbonyl group is removed to form $C_8H_{14}O_7$ with lower DBE, whose path is similar with Liu's work [63]. The distribution of KMD(CO2) is similar to that of KMD(CO), but it shows that the removal of carboxyl groups in the secondary reaction only take place in sugars and phenolic-like species.

Many solid points appeared in different KMD diagrams, indicating that these substances might act as intermediates with different reaction paths for different substances production in the evolution of heavy compounds. At the same time, some primary pyrolysis products are not collinear with any products of secondary reaction, which means these products undergo more complex reactions in the secondary reaction step, such as ring opening, carbon chain cleavage, etc.

Fig. 10 illustrates the evolution of oxygen atoms replacing the molecular weight with the number of oxygen atoms in KMD diagram. The dehydration and decarbonylation reactions mainly take place for substances with ON $<$ 10 in the secondary reaction stage, while only few substances with ON $>$ 10 undergo deoxidation, indicating that the compounds with large ON mainly experience more complex reactions during the secondary reaction.

3.3.3. *Evolution of hemicellulose-derived heavy compounds*

Compared with cellulose, the hemicellulose-derived heavy compounds in two-stage pyrolysis widely overlap in the "main line" region, which indicates that the pyrolysis process of hemicellulose is dominated by homologue evolution, assisted with some cleavage of carbon chain or other complex reactions.

In the KMD(CH2) diagram, just like cellulose, a part of lipids and unsaturated hydrocarbons generated by the growth of alkane chains also appear outside the "main line", like $C_{31}H_{40}O_3$ and $C_{35}H_{48}O_3$ shown in Fig. 11. In KMD(H2O), it is observed that the dehydration reaction occurs mainly in sugars and phenolic-like species but less in lipids and unsaturated hydrocarbons, which is different from those of cellulose. This result indicated that nearly no oxygen atoms existed in the lipids and unsaturated hydrocarbons in the form of hydroxyl groups. The KMD (CO) and KMD(CO2) figures show that the removal of carbonyl and carboxyl groups also occur in sugars, phenolic-like species and condensed aromatic hydrocarbons, while these reactions hardly take place in unsaturated hydrocarbons and lipid. Meanwhile, the removal reaction of CO_2 is much weaker than that of CO in the secondary reaction of hemicellulose. It was indicated in previous study that many carboxylic groups were intermolecularly dehydrated while lots of C═O bond were retained at the ends of small pyrolytic fragments [64], which explained the stronger removal of CO in the secondary reaction. The variation of KMD with the ON in Fig. 12 shows that the hemicellulose-derived substances with large ON in the heavy compounds transform into lower ON compounds mainly through dehydration and decarbonylation during the secondary reactions.

3.3.4. *Evolution of lignin-derived heavy compounds*

Due to the abundant of methyl or methoxy side chains in the lignin units [65], the changes of OCH_2 groups are also considered in addition to CH_2, H_2O, CO and CO_2 groups introduced above. As shown in Fig. 13, lignin generates varieties of products during the primary stage of pyrolysis. As the reaction time increase, many non-collinear products appear. The homologous evolution of lignin-derived compounds in the "main line" region is not as strong as that of cellulose and hemicellulose, but obviously more active in the unsaturated hydrocarbons and lipids in outside region. This finding suggests that the heavy components of lignin tended to be cracked or condensed in the secondary reaction.

The KMD(CH2) diagram in Fig. 13 indicates that the alkane chain growth mainly takes place in the unsaturated hydrocarbons, lipids and phenolic substances. Some phenylpropanes detected by GCMS and FTMS showed the evolution caused by multi-stage demethylation (KMD (CH2) = 0.12243). In addition, the phenolic substances produced during lignin pyrolysis experience the removal of OCH_2 groups, CO groups and a few H_2O groups attributed to the abundant sidechains. However, the removal of CO is more intensive than that of H_2O, and both of them take place on the propylene or propanol sidechains [65,66]. This indicates that the oxygen-contained groups on the propyl sidechains are mainly present in the form of C═O. The dehydration reaction takes place in the lipids, which probably due to the involvement of fragments containing hydroxyl side chains during the recombination. At the same time, some lipids and unsaturated hydrocarbons also undergo the removal of OCH_2 groups (seen in KMD(OCH2)). This could be attributed to the presence of methoxy benzene side chains of these substances or the involvement of hydroxymethyl fragments during the formation of lipids and unsaturated hydrocarbons. The KMD(CO) figure shows that the CO removal only occurs in lipids and some phenolic substances. It should be pointed out that there is almost no compounds collinear in the KMD(CO2) figure, consequently, the KMD(CO2) figure of lignin is omitted here. Moreover, this result also proves that C═O in lignin heavy compounds mainly exist

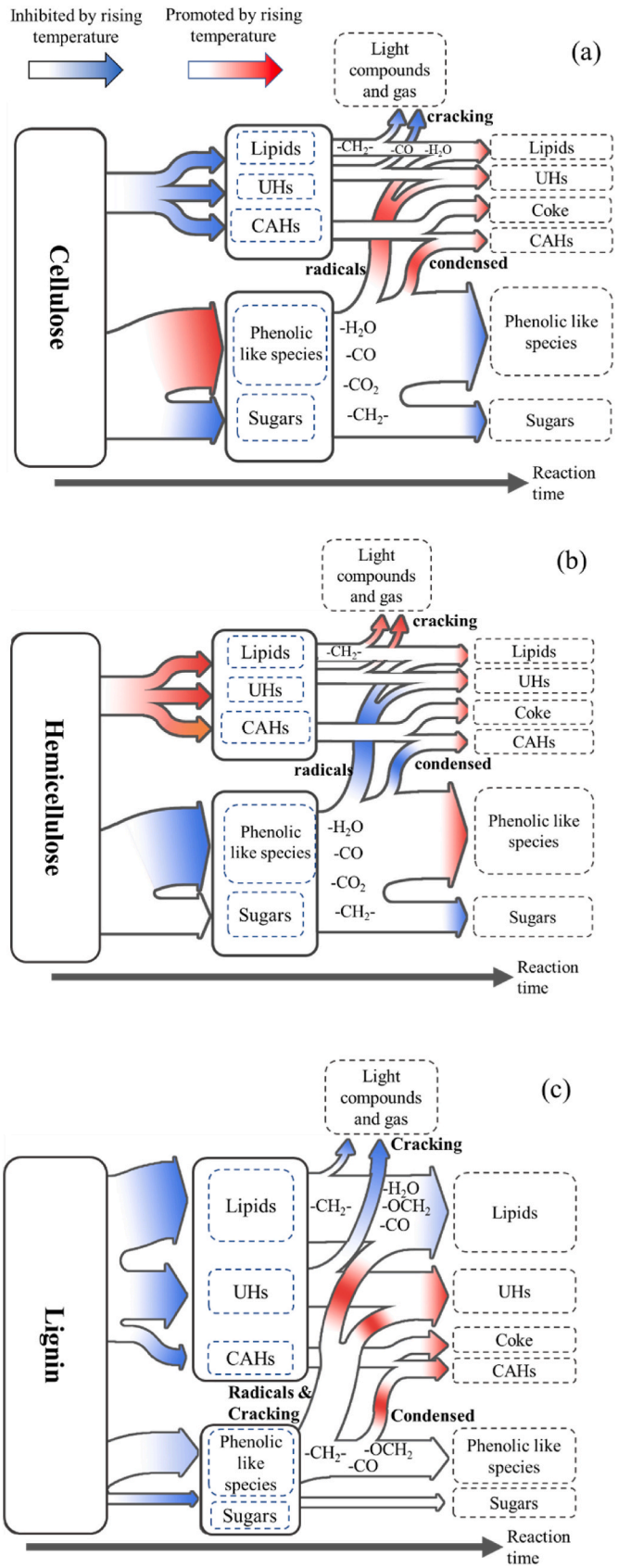

Fig. 15. The evolution of heavy compounds derived from three main components of biomass : (a) Cellulose, (b) Hemicellulose and (c) Lignin. UHs represents unsaturated hydrocarbons and CAHs represents condensed aromatic hydrocarbons.

in the form of aldehyde or ketone.

Fig. 14 shows that the evolution of oxygen-contained heavy compounds of lignin is far more complicated than these homologous transformations, and there are more unstable structures with large molecular weight resulting from a lot of complex cleavage and condensation.

3.4. Evolution routes of heavy bio-oil compounds

The heavy components derived from pyrolysis of the three components at 500, 600 and 700 °C with different reaction times have been analyzed in the previous sections. From these results, the possible evolution routes of the heavy components are shown in Fig. 15. All the five kinds of species (classified in section 3.2.1) are already generated during the primary pyrolysis. The lipids and phenolic-like species are dominant in lignin-derived and cellulose/hemicellulose-derived heavy oil, respectively. Then during the secondary reaction stage, the phenolic-like species and sugars are the most active components that undergo cracking, condensation and homologous evolution (–CH_2–, –CO, –CO_2, –H_2O, –OCH_2). Most of lipids and unsaturated hydrocarbons (UHs) are produced by the recombination of radicals generated by the secondary reactions of phenolic-like species and sugars. These possible routes of evolution, especially the formation of lipids and UHs, are differently affected by temperature (500,600 and 700 °C). Generally, high temperatures promote the formation of these two species in secondary reactions of cellulose and hemicellulose while inhibiting those of lignin.

4. Conclusion

The species and abundance of heavy components change greatly with temperature in different pyrolysis stages. The increase in temperature promotes the pyrolysis of phenolic-like species and sugars, and facilitates the formation of other species in cellulose pyrolysis oil. For hemicellulose, a temperature increase accelerates the pyrolysis process and inhibits the secondary reactions of its phenolic-like species. The formation of lipids, unsaturated hydrocarbons and condensed aromatic hydrocarbons during the primary pyrolysis of lignin are inhibited by the temperature increase. However, it tends to promote their formation during the secondary reaction step. KMD results show that there are two pathways for the evolution of heavy components: homologous evolution and complex cracking or condensation. With the increase of reaction time, heavy components of cellulose and hemicellulose mainly undergo homologous evolution, which is achieved through dehydration, decarbonylation, and mildly decarboxylation. The lipids and some unsaturated hydrocarbons produced during the secondary pyrolysis mainly form by growth of alkane chains. Many other complex reactions like cracking and condensation happen during secondary pyrolysis of lignin-derived heavy compounds because of its unstable structure. This work is intended to bring new insights in the conversion mechanisms of cellulose, hemicellulose and lignin in pyrolysis.

Credit author statement

Dian Zhong: Writing – original draft, Software, Visualization, Kuo Zeng: Writing – review & editing, Methodology, Formal analysis, Jun Li: Investigation, Formal analysis, Visualization, Yi Qiu: Resources, Gilles Flamant: Methodology, Formal analysis, Ange Nzihou: Investigation, Formal analysis, Visualization, Vasilevich Sergey Vladimirovich: Formal analysis, Polishing language, Haiping Yang: Conceptualization, Resources, Validation, Hanping Chen: Validation.

Declaration of competing interest

The authors declare that they have no known competing financial interests or personal relationships that could have appeared to influence the work reported in this paper.

Acknowledgement

Authors acknowledge funding from the National Key R&D Program of China (2017YFE0124200), the National Natural Science Foundation of China (52076098), the International Cooperation Project of Shenzhen (GJHZ20190820102607238) and the Young Top-notch Talent Cultivation Program of Hubei Province. There are no conflicts to declare.

Appendix A. Supplementary data

Supplementary data to this article can be found online at https://doi.org/10.1016/j.rser.2021.111989.

References

[1] Hu X, Gholizadeh M. Progress of the applications of bio-oil. Renew Sustain Energy Rev 2020;134:110124. https://doi.org/10.1016/j.rser.2020.110124.
[2] Sepehri A, Sarrafzadeh M-H. Effect of nitrifiers community on fouling mitigation and nitrification efficiency in a membrane bioreactor. Chem. Eng. Process. Process Intensific. 2018;128:10–8. https://doi.org/10.1016/j.cep.2018.04.006.
[3] Sepehri A, Sarrafzadeh M-H, Avateffazeli M. Interaction between Chlorella vulgaris and nitrifying-enriched activated sludge in the treatment of wastewater with low C/N ratio. J Clean Prod 2020;247:119164. https://doi.org/10.1016/j.jclepro.2019.119164.
[4] Oasmaa A, Peacocke C. A guide to physical property characterisation of biomass-derived fast pyrolysis liquids, vol. 450. VTT Publications; 2001. p. 2–65.
[5] Yu H, Zhang Z, Li Z, Chen D. Characteristics of tar formation during cellulose, hemicellulose and lignin gasification. Fuel 2014;118:250–6. https://doi.org/10.1016/j.fuel.2013.10.080.
[6] Yang H, Yan R, Chen H, Zheng C, Lee DH, Liang DT. In-depth investigation of biomass pyrolysis based on three major components: hemicellulose, cellulose and lignin. Energy Fuel 2006;20:388–93. https://doi.org/10.1021/ef0580117.
[7] Demirbas A. Competitive liquid biofuels from biomass. Appl Energy 2011;88:17–28. https://doi.org/10.1016/j.apenergy.2010.07.016.
[8] Bradbury AGW, Sakai Y, Shafizadeh F. A kinetic model for pyrolysis of cellulose. J Appl Polym Sci 1979;23:3271–80. https://doi.org/10.1002/app.1979.070231112.
[9] Vinu R, Broadbelt LJ. A mechanistic model of fast pyrolysis of glucose-based carbohydrates to predict bio-oil composition. Energy Environ Sci 2012;5:9808. https://doi.org/10.1039/c2ee22784c.
[10] Mettler MS, Mushrif SH, Paulsen AD, Javadekar AD, Vlachos DG, Dauenhauer PJ. Revealing pyrolysis chemistry for biofuels production: conversion of cellulose to furans and small oxygenates. Energy Environ Sci 2012;5:5414–24. https://doi.org/10.1039/C1EE02743C.
[11] Lu Q, Yang X, Dong C, Zhang Z, Zhang X, Zhu X. Influence of pyrolysis temperature and time on the cellulose fast pyrolysis products: analytical Py-GC/MS study. J Anal Appl Pyrol 2011;92:430–8. https://doi.org/10.1016/j.jaap.2011.08.006.
[12] Hosoya T, Kawamoto H, Saka S. Different pyrolytic pathways of levoglucosan in vapor- and liquid/solid-phases. J Anal Appl Pyrol 2008;83:64–70. https://doi.org/10.1016/j.jaap.2008.06.008.
[13] Hosoya T, Kawamoto H, Saka S. Solid/liquid- and vapor-phase interactions between cellulose- and lignin-derived pyrolysis products. J Anal Appl Pyrol 2009;85:237–46. https://doi.org/10.1016/j.jaap.2008.11.028.
[14] Hosoya T, Kawamoto H, Saka S. Pyrolysis gasification reactivities of primary tar and char fractions from cellulose and lignin as studied with a closed ampoule reactor. J Anal Appl Pyrol 2008;83:71–7. https://doi.org/10.1016/j.jaap.2008.06.002.
[15] Chen WH, Wang CW, Ong HC, Show PL, Hsieh TH. Torrefaction, Pyrolysis and Two-stage Thermodegradation of Hemicellulose, Cellulose and Lignin. Fuel 2019;258:116168. https://doi.org/10.1016/j.fuel.2019.116168.
[16] Fisher T, Hajaligol M, Waymack B, Kellogg D. Pyrolysis behavior and kinetics of biomass derived materials. J Anal Appl Pyrol 2002;62:331–49. https://doi.org/10.1016/S0165-2370(01)00129-2.
[17] Ponder GR, Richards GN. Thermal synthesis and pyrolysis of a xylan. Carbohydr Res 1991;218:143–55. https://doi.org/10.1016/0008-6215(91)84093-T.
[18] Shen DK, Gu S, Bridgwater AV. The thermal performance of the polysaccharides extracted from hardwood: cellulose and hemicellulose. Carbohydr Polym 2010;82:39–45. https://doi.org/10.1016/j.carbpol.2010.04.018.
[19] Yang H, Yan R, Chen H, Lee DH, Zheng C. Characteristics of hemicellulose, cellulose and lignin pyrolysis. Fuel 2007;86:1781–8. https://doi.org/10.1016/j.fuel.2006.12.013.
[20] Kawamoto H, Horigoshi S, Saka S. Pyrolysis reactions of various lignin model dimers. J Wood Sci 2007;53:168–74. https://doi.org/10.1007/s10086-006-0834-z.
[21] Patwardhan PR, Brown RC, Shanks BH. Understanding the fast pyrolysis of lignin. ChemSusChem 2011;4:1629–36. https://doi.org/10.1002/cssc.201100133.
[22] Xiao L, Hu S, Han H, Ren Q, He L, Jiang L, et al. An insight into the OPAHs and SPAHs formation mechanisms during alkaline lignin pyrolysis at different temperatures. J Anal Appl Pyrol 2021;156. https://doi.org/10.1016/j.jaap.2021.105104.
[23] Hua W, Jing L, Hongling Y, Xiangqiong Z, Lingbo L, Tianhui R. The tribological behavior of diester-containing polysulfides as additives in mineral oil. Tribol Int 2007;40:1246–52. https://doi.org/10.1016/j.triboint.2007.01.024.
[24] Hertzog J, Carré V, Le Brech Y, Dufour A, Aubriet F. Toward controlled ionization conditions for ESI-FT-ICR-MS analysis of bio-oils from lignocellulosic material. Energy Fuel 2016;30:5729–39. https://doi.org/10.1021/acs.energyfuels.6b00655.
[25] Terrell E, Garcia-Perez M. Novel strategy to analyze fourier transform ion cyclotron resonance mass spectrometry data of biomass pyrolysis oil for oligomeric structure assignment. Energy Fuel 2020;34:8466–81. https://doi.org/10.1021/acs.energyfuels.0c01687.
[26] Liu Y, Shi Q, Zhang Y, He Y, Chung KH, Zhao S, et al. Characterization of red pine pyrolysis bio-oil by gas chromatography–mass spectrometry and negative-ion electrospray ionization fourier transform ion cyclotron resonance mass spectrometry. Energy Fuel 2012;26:4532–9. https://doi.org/10.1021/ef300501t.
[27] Xiong Z, Han H, Azis MM, Hu X, Wang Y, Su S, et al. Formation of the heavy tar during bio-oil pyrolysis: a study based on Fourier transform ion cyclotron resonance mass spectrometry. Fuel 2019;239:108–16. https://doi.org/10.1016/j.fuel.2018.10.151.
[28] Xiong Z, Guo J, Chaiwat W, Deng W, Hu X, Han H, et al. Assessing the chemical composition of heavy components in bio-oils from the pyrolysis of cellulose, hemicellulose and lignin at slow and fast heating rates. Fuel Process Technol 2020;199:106299. https://doi.org/10.1016/j.fuproc.2019.106299.
[29] Xiao L, Hu S, Song Y, Zhang L, Han H, Liu C, et al. The formation mechanism for OPAHs during the cellulose thermal conversion in inert atmosphere at different temperatures based on ESI(−) FT-ICR MS measurement and density functional theory (DFT). Fuel 2019;239:320–9. https://doi.org/10.1016/j.fuel.2018.10.113.
[30] Bai X, Kim KH, Brown RC, Dalluge E, Hutchinson C, Lee YJ, et al. Formation of phenolic oligomers during fast pyrolysis of lignin. Fuel 2014;128:170–9. https://doi.org/10.1016/j.fuel.2014.03.013.
[31] Zhang R, Qi Y, Ma C, Ge J, Hu Q, Yue F-J, et al. Characterization of lignin compounds at the molecular level: mass spectrometry analysis and raw data processing. Molecules 2021;26:178. https://doi.org/10.3390/molecules26010178.
[32] Qi Y, Hempelmann R, Volmer DA. Two-dimensional mass defect matrix plots for mapping genealogical links in mixtures of lignin depolymerisation products. Anal Bioanal Chem 2016;408:4835–43. https://doi.org/10.1007/s00216-016-9598-5.
[33] Dhungana B, Becker C, Zekavat B, Solouki T, Hockaday WC, Chambliss CK. Characterization of slow-pyrolysis bio-oils by high-resolution mass spectrometry and ion mobility spectrometry. Energy Fuel 2015;29:744–53. https://doi.org/10.1021/ef5016389.
[34] Jiang W, Chu J, Wu S, Lucia LA. Modeling pyrolytic behavior of pre-oxidized lignin using four representative β-ether-type lignin-like model polymers. Fuel Process Technol 2018;176:221–9. https://doi.org/10.1016/j.fuproc.2018.03.041.
[35] Deng J, Xiong T, Wang H, Zheng A, Wang Y. Effects of cellulose, hemicellulose, and lignin on the structure and morphology of porous carbons. ACS Sustainable Chem Eng 2016;4:3750–6. https://doi.org/10.1021/acssuschemeng.6b00388.
[36] Xiong Z, Xiong Y, Li Q, Han H, Deng W, Xu J, et al. Effects of vapor-/solid-phase interactions among cellulose, hemicellulose and lignin on the formation of heavy components in bio-oil during pyrolysis. Fuel Process Technol 2022;225:107042. https://doi.org/10.1016/j.fuproc.2021.107042.
[37] Xiong Z, Guo J, Han H, Xu J, Jiang L, Su S, et al. Effects of AAEMs on formation of heavy components in bio-oil during pyrolysis at various temperatures and heating rates. Fuel Process Technol 2021;213:106690. https://doi.org/10.1016/j.fuproc.2020.106690.
[38] Xiong Z, Jiang L, Xu J, Li Q, Deng W, Su S, et al. Effects of the gas-/liquid-phase interactions on the evolution of bio-oil during its thermal treatment. Energy Fuel 2020;34:8482–92. https://doi.org/10.1021/acs.energyfuels.0c01811.
[39] Li J, Xiong Z, Zeng K, Zhong D, Zhang X, Chen W, et al. Characteristics and evolution of nitrogen in the heavy components of algae pyrolysis bio-oil. Environ Sci Technol 2021;55:6373–85. https://doi.org/10.1021/acs.est.1c00676.
[40] Yue H, Vieth-Hillebrand A, Han Y, Horsfield B, Schleicher AM, Poetz S. Unravelling the impact of lithofacies on the composition of NSO compounds in residual and expelled fluids of the Barnett, Niobrara and Posidonia formations. Org Geochem 2021;155:104225. https://doi.org/10.1016/j.orggeochem.2021.104225.
[41] Staš M, Chudoba J, Auersvald M, Kubička D, Conrad S, Schulzke T, et al. Application of orbitrap mass spectrometry for analysis of model bio-oil compounds and fast pyrolysis bio-oils from different biomass sources. J Anal Appl Pyrol 2017;124:230–8. https://doi.org/10.1016/j.jaap.2017.02.002.
[42] Miettinen I, Mäkinen M, Vilppo T, Jänis J. Compositional characterization of phase-separated pine wood slow pyrolysis oil by negative-ion electrospray ionization fourier transform ion cyclotron resonance mass spectrometry. Energy Fuel 2015;29:1758–65. https://doi.org/10.1021/ef5025966.
[43] Wang J, Hao Z, Shi F, Yin Y, Cao D, Yao Z, et al. Characterization of brominated disinfection byproducts formed during the chlorination of aquaculture seawater. Environ Sci Technol 2018;52:5662–70. https://doi.org/10.1021/acs.est.7b05331.
[44] Ohno T, Ohno PE. Influence of heteroatom pre-selection on the molecular formula assignment of soil organic matter components determined by ultrahigh resolution mass spectrometry. Anal Bioanal Chem 2013;405:3299–306. https://doi.org/10.1007/s00216-013-6734-3.
[45] Koch BP, Witt M, Engbrodt R, Dittmar T, Kattner G. Molecular formulae of marine and terrigenous dissolved organic matter detected by electrospray ionization Fourier transform ion cyclotron resonance mass spectrometry. Geochem Cosmochim Acta 2005;69:3299–308. https://doi.org/10.1016/j.gca.2005.02.027.
[46] Koch BP, Dittmar T, Witt M, Kattner G. Fundamentals of molecular formula assignment to ultrahigh resolution mass data of natural organic matter. Anal Chem 2007;79:1758–63. https://doi.org/10.1021/ac061949s.
[47] Kendrick E. A mass scale based on CH 2 = 14.0000 for high resolution mass spectrometry of organic compounds. Anal Chem 1963;35:2146–54. https://doi.org/10.1021/ac60206a048.

[48] Dier TKF, Egele K, Fossog V, Hempelmann R, Volmer DA. Enhanced mass defect filtering to simplify and classify complex mixtures of lignin degradation products. Anal Chem 2016;88:1328–35. https://doi.org/10.1021/acs.analchem.5b03790.
[49] Roach PJ, Laskin J, Laskin A. Higher-order mass defect analysis for mass spectra of complex organic mixtures. Anal Chem 2011;83:4924–9. https://doi.org/10.1021/ac200654j.
[50] Kilgour DPA, Mackay CL, Langridge-Smith PRR, O'Connor PB. Appropriate degree of trust: deriving confidence metrics for automatic peak assignment in high-resolution mass spectrometry. Anal Chem 2012;84:7431–5. https://doi.org/10.1021/ac301339d.
[51] Hughey CA, Hendrickson CL, Rodgers RP, Marshall AG, Qian K. Kendrick mass defect spectrum: a compact visual analysis for ultrahigh-resolution broadband mass spectra. Anal Chem 2001;73:4676–81. https://doi.org/10.1021/ac010560w.
[52] Lanza R, Dalle Nogare D, Canu P. Gas phase chemistry in cellulose fast pyrolysis. Ind Eng Chem Res 2009;48:1391–9. https://doi.org/10.1021/ie801280g.
[53] Shen DK, Gu S. The mechanism for thermal decomposition of cellulose and its main products. Bioresour Technol 2009;100:6496–504. https://doi.org/10.1016/j.biortech.2009.06.095.
[54] Xin S, Yang H, Chen Y, Wang X, Chen H. Assessment of pyrolysis polygeneration of biomass based on major components: product characterization and elucidation of degradation pathways. Fuel 2013;113:266–73. https://doi.org/10.1016/j.fuel.2013.05.061.
[55] He Z, Guo M, Sleighter RL, Zhang H, Chanel F, Hatcher PG. Characterization of defatted cottonseed meal-derived pyrolysis bio-oil by ultrahigh resolution electrospray ionization Fourier transform ion cyclotron resonance mass spectrometry. J Anal Appl Pyrol 2018;136:96–106. https://doi.org/10.1016/j.jaap.2018.10.018.
[56] Mann BF, Chen H, Herndon EM, Chu RK, Tolic N, Portier EF, et al. Indexing permafrost soil organic matter degradation using high-resolution mass spectrometry. PLoS One 2015;10:e0130557. https://doi.org/10.1371/journal.pone.0130557.
[57] Wang Q, Song H, Pan S, Dong N, Wang X, Sun S. Initial pyrolysis mechanism and product formation of cellulose: an Experimental and Density functional theory (DFT) study. Sci Rep 2020;10:1–18. https://doi.org/10.1038/s41598-020-60095-2.
[58] Scheer AM, Mukarakate C, Robichaud DJ, Ellison GB, Nimlos MR. Radical chemistry in the thermal decomposition of anisole and deuterated anisoles: an investigation of aromatic growth. J Phys Chem 2010;114:9043–56. https://doi.org/10.1021/jp102046p.
[59] Kawamoto H. Review of reactions and molecular mechanisms in cellulose pyrolysis. Curr Org Chem 2016;20:1. https://doi.org/10.2174/2213337203666160525102910.
[60] Wang S, Liang T, Ru B, Guo X. Mechanism of xylan pyrolysis by Py-GC/MS. Chem Res Chin Univ 2013;29:782–7. https://doi.org/10.1007/s40242-013-2447-6.
[61] Hosoya T, Kawamoto H, Saka S. Role of methoxyl group in char formation from lignin-related compounds. J Anal Appl Pyrol 2009;84:79–83. https://doi.org/10.1016/j.jaap.2008.10.024.
[62] Stankovikj F, McDonald AG, Helms GL, Garcia-Perez M. Quantification of bio-oil functional groups and evidences of the presence of pyrolytic humins. Energy Fuel 2016;30:6505–24. https://doi.org/10.1021/acs.energyfuels.6b01242.
[63] Liu C, Huang J, Huang X, Li H, Zhang Z. Theoretical studies on formation mechanisms of CO and CO2in cellulose pyrolysis. Comput. Theor. Chem. 2011;964:207–12. https://doi.org/10.1016/j.comptc.2010.12.027.
[64] Yang X, Zhao Y, Li W, Li R, Wu Y. Unveiling the pyrolysis mechanisms of hemicellulose: experimental and theoretical studies. Energy Fuel 2019;33:4352–60. https://doi.org/10.1021/acs.energyfuels.9b00482.
[65] Shen Q, Fu Z, Li R, Wu Y. A study on the pyrolysis mechanism of a β-O-4 lignin dimer model compound using DFT combined with Py-GC/MS. J Therm Anal Calorim 2021;146:1751–61. https://doi.org/10.1007/s10973-020-10130-1.
[66] Kawamoto H. Lignin pyrolysis reactions. J Wood Sci 2017;63:117–32. https://doi.org/10.1007/s10086-016-1606-z.